Journal of Analytical and Applied Pyrolysis, Vol. 130, March 2018, pp. 127-134
DOI:10.1016/j.jaap.2018.01.018

Influence of temperature and particle size on structural characteristics of chars from Beechwood pyrolysis

Jie Yu[1,2], Lushi Sun[1,2], César Berrueco[2,3], Beatriz Fidalgo[2,4], Nigel Paterson[2], Marcos Millan[2*]

[1] State Key Laboratory of Coal Combustion, Huazhong University of Science and Technology, Wuhan, Hubei 430074, China

[2] Department of Chemical Engineering, Imperial College, London SW7 2AZ, UK

[3] Current Address: Catalonia Institute for Energy Research, IREC. C/ Marcel·lí Domingo, 2. 43007 Tarragona, Spain

[4] Current Address: Bioenergy and Resource Management Centre, Cranfield University, Cranfield MK43 0AL, UK

* Corresponding author. Tel.: +44(0)2079541633

E-mail address: marcos.millan@imperial.ac.uk

Abstract

This work investigates the effect of temperature and particle size on the product yields and structure of chars obtained from the pyrolysis of Beechwood Chips (BWC), a lignocellulosic biomass. BWC of three different size fractions (0.21-0.50 mm, 0.85-1.70 mm and 2.06-3.15 mm) were pyrolyzed at atmospheric pressure and temperatures ranging from 300 to 900 °C in a fixed bed reactor. Tar and gas yields increased with increasing temperature, while char yield decreased, particularly between 300 and 450 °C. The effect of particle size was mostly observed at temperatures lower than 400 °C as a larger char yield for larger particles due to intraparticle reactions. At higher temperatures the larger surface area in the char fixed bed favoured reactions increasing char and gas yields from the smaller particles. Pyrolysis chars were characterized using Fourier transform infrared spectroscopy (FTIR), X-ray diffraction (XRD) and Raman spectroscopy. Loss in oxygenated functional groups and aliphatic side chains with increasing temperature was revealed, along with an increase in the concentration of large aromatic systems, leading to a more ordered char structure but no significant graphitization. The changes in char nature at high temperature led to a loss in their combustion reactivity. Raman spectra indicated that the temperature needed to completely decompose the cellulose structure increased with biomass particle size and the enhanced intraparticle reactions in pyrolysis of large particles was likely to give rise to amorphous carbon structures with small fused ring systems.

Keywords: Biomass pyrolysis; FTIR; XRD; Raman; Reactivity

1. Introduction

Biomass as a renewable fuel resource for energy production is likely to play a major role to replace fossil fuels, help meet the increasing energy demand and reduce CO_2 emissions. Pyrolysis is not only the first set of reactions undergone by biomass in combustion and gasification [1,2], but it can also be an effective process to produce a solid fuel without the large amount of oxygen and moisture present in the biomass, which reduce its heating value and represent a drawback to its use.

Therefore, the study of pyrolysis is of great importance, not only because it affects the yields of the pyrolysis products, but also the char reactivity in subsequent processes [3-7]. Among the various uses of chars from biomass pyrolysis a route, to a char that can be used as a substitute to pulverized coal in steelmaking in electric arc furnaces has recently been reported [8]. The suitability of biomass-derived char for electric arc furnace applications depends on its structure, heating value and reactivity, which are all affected by the pyrolysis process.

The influence of biomass pyrolysis operating conditions on the developing char structure caused by the release of volatiles from the biomass matrix has been the subject of several studies [3,4,6,7]. Generally, smaller particle size and higher heating rate leads to less char yields. Temperature has a great effect on char yields and properties [5]. The structural properties of a char are determined by the parent biomass and pyrolysis operating variables, such as heating rate, peak temperature, residence time and particle size, and the type of pyrolyser, as there can be significant differences between chars from fixed beds, fluidized beds and entrained flow reactors [9,10]. These variables affect char reactivity due to their effect on elemental composition, functional groups, surface area, carbon microstructure, and agglomeration of inorganic matter, which plays a catalytic role in gasification and combustion.

Biomass grinding into the small particle sizes required for many applications is energy intensive. Therefore, selecting an appropriate biomass particle size has an impact on process economics. Understanding the effect of pyrolysis temperature and particle size on the structure of chars is useful to select and optimize pyrolysis conditions to produce high quality chars for different processes, including their use in electric arc furnaces. Hence, the present work investigates the combined effect of temperature and particle size on the product yields and char structure from BWC pyrolysis. A novel adaptation of a Gray King (GK) apparatus has been used to produce chars. This configuration enables an assessment of the extent of reactions of the evolving volatiles both intraparticle (before volatiles

are released from a particle) and interparticle (where volatiles generated in one particle react over other particles in the bed). Structural characteristics of raw biomass and the biomass chars are studied by a range of advanced analytical methods to investigate changes in char structure with conditions of formation. FTIR, XRD and Raman spectroscopy provide an insight into char structures [7,11-18], and the influence of char structural changes on combustion reactivity has been investigated by thermogravimetric analysis.

2. Experimental Section

2.1 Sample preparation

A sample of BWC was ground by a biomass shredder and sieved to three different particle size fractions: 0.21-0.50 mm, 0.85-1.70 mm and 2.06-3.15 mm. Before each experiment, the samples were placed in a vacuum oven, dried overnight at 35 °C and then stored in a desiccator cabinet until used. Elemental analysis of the samples was carried out using a Vario EL-2 elemental analyzer. Proximate analysis (TGA2000, Las Navas) was conducted to determine moisture, volatile matter, fixed carbon, and ash contents. Approximately 3–4 mg of sample was heated to 50 °C and held at that temperature for 10 min under N_2 atmosphere (40 mL min^{-1}). Afterwards, temperature was increased in two steps: (i) to 110 °C at 10 °C min^{-1} and held for 30 min in order to record moisture; (ii) to 900 °C at 10 °C min^{-1} and held for 30 min to measure volatile matter contents. Temperature was then decreased to 800 °C at 10 °C min^{-1} and held for 10 min under the same flowrate of N_2. Next, the sweep gas was switched to air (40 mL min^{-1}) and held for 40 min in order to register fixed carbon and ash contents. The detailed analysis of the BWC sample is shown in Table 1.

2.2 Pyrolysis set-up and procedure

A laboratory scale quartz reactor (length: 300 mm, inner diameter: 20 mm) was set up in a fixed bed configuration for this study according to the layout shown in Figure 1. This reactor was adapted from the standard Gray-King assay test [19]. For each run, 2-3 g of BWC was placed in a wire mesh cage inside the quartz tube reactor at room temperature and heated, by means of a furnace, to the pyrolysis peak temperature, at a heating rate of about 50 °C min^{-1}. Several temperatures in the range 300 and 900 °C were evaluated. Once the peak temperature was achieved, it was kept constant for 15 minutes before the quartz reactor was removed from the furnace and allowed to cool. Two thermocouples were used to monitor temperature at the front and rear of the biomass bed. A flow rate of 1.2 L min^{-1} of helium was used to sweep the volatile products out of the reactor and into the tar trap. The tar trap was

composed of a glass U-tube immersed in a liquid nitrogen bath, which condensed most of the tar. An external cotton-filled filter was placed downstream from the tar trap to remove any residual tar mist. The tar collected in the cold trap system was formed over a temperature range from the onset of volatile release up to the peak temperature. The primary char in the cage and tar in the U-tube and tar trap system filter were the main recovered products at the end of each pyrolysis run. Only traces of tar and secondary char were observed in the reactor outlet tube section. The solid residues were collected and weighed to calculate the char yield as a percentage of the initial biomass weight. Tar yield was calculated from the difference in weight between the tar trap system and reactor before and after each run and reported as a percentage of the initial biomass weight. Gas yield was calculated by difference.

2.3 Characterization of Chars and Tars

XRD spectra of the char samples were obtained using a PANalytical B.V. X'Pert Pro multipurpose X-ray diffractometer (40 mA, 40 kV, Cu KR). Samples were scanned in a step-scan mode with a step size of 0.01° over an angular 2θ range of 10-90°. The apparent microcrystallite diameters (La) were calculated using Warren's formula [20]:

$$\mathrm{La} = \frac{1.84\lambda}{\mathrm{B}\cos(\theta)}$$

where λ is the X-ray wavelength, θ is the Bragg angle and B is the breadth at half-maximum intensity in radians.

The main organic functional groups in the char particles were analyzed using an FTIR spectrometer (Bruker, VERTEX 70, Germany). The samples were first powdered in an agate mortar and then mixed with KBr to prepare transparent wafers. The mixture of char and KBr powder was dried overnight in an oven at 105 °C. FTIR spectra were obtained with 4 cm^{-1} resolution and 32 scans between 4000 and 400 cm^{-1}.

Raman measurements were conducted with a Confocal Raman Microspectroscope (Type: Renishaw RM-1000), using an Ar+ laser beam at 514.4 nm, with spectral resolution 1 cm^{-1} and laser power of less than 0.4 mW (at the samples) was used as an excitation source. Raman spectra were measured in the range of 800-1800 cm^{-1}.

A Perkin–Elmer Thermogravimetric Analyser (TGA) Pyris 1 was used to determine combustion reactivity of biomass chars. Approximately 2-3 mg of solid sample were heated from 50 to 400 °C at a heating rate of 50 °C min in an inert N_2 atmosphere (40 mL min^{-1}). Next, the sweep gas was

switched to air (40 mL min^{-1}) for the combustion reaction and temperature was increased at a rate of 15 °C min^{-1} to 900 °C and held for 5 min. Half-life temperature ($T_{50\%}$) and maximum reactivity temperature (T_{Rmax}) were determined from the TGA data as char reactivity indices. $T_{50\%}$ is defined as the temperature at which 50% of the combustible material has reacted. The T_{Rmax} is the temperature at which the weight loss rate presents its maximum. Shifts of these values towards higher temperatures indicate lower sample reactivity.

Molecular size distributions of the tars were compared by size exclusion chromatography (SEC) analysis carried out using a 300 mm long, 7.5 mm i.d., polystyrene/polydivinylbenzene-packed, Mixed-D column (Polymer Laboratories, U.K.). The chromatograph was operated at 80 ºC and 1-methyl-2-pyrrolidinone (NMP) as the mobile phase with a flow rate of 0.5 mL min^{-1}. Signal detection was carried out using a Knauer diode array Smartline 2600 detector, with UV absorbance at 300 nm.

3. Results and Discussion

3.1. Effect of operating conditions on product yields

In these pyrolysis tests the samples were heated at a rate of approximately 50 °C min^{-1} and subsequently held for 15 minutes at peak temperatures between 300 and 900 °C. Tar and gas were therefore partially released during the heating ramp and their release continued towards completion at the peak temperature. Similarly, char began to form during the heating ramp, and continued to form and develop its final structure in the isothermal step.

3.1.1. Effect of temperature

Figure 2 shows the char, tar and gas yields from the pyrolysis of BWC as a function of peak temperature (325 to 900 °C) for three particle size ranges (0.21-0.50 mm, 0.85-1.70 mm and 2.06-3.15 mm). As can be seen, temperature had a significant effect on product yields, particularly in the range from 300 to 450 °C, where increases in temperature led to an increase in gas and tar production and a rapid decrease in the char yield. The sharp changes in product yields between 300 and 450 °C are consistent with previous work on the pyrolysis of the biomass constituents, cellulose, xylan and lignin. According to that study, thermal degradation or depolymerisation of hemicellulose, cellulose and lignin mainly occurs in the intervals 225~400 °C, 325~425 °C and 250~500 °C, respectively, while their corresponding temperatures of maximum pyrolysis rates are 275 to 325 °C for hemicellulose, and 375 °C for lignin and cellulose [21].

This explains the relatively large char yields obtained in this work at lower temperatures (325 and 350 °C), as the maximum rates of cellulose and lignin decomposition had not been reached. As temperature was raised to between 350 and 400 °C, a region in which most cellulose, as well as a significant fraction of lignin, depolymerise, the release of volatiles was favoured and a large char yield drop was observed. The sharp decrease in the yield slopes above approximately 450 °C shows that the release of volatiles was virtually complete at this temperature within the residence time of the test. As temperature increased further above 450 °C only a slight decrease in char yield was observed, probably due to char rearrangements, in line with the small changes in char yields of hemicellulose and lignin observed in previous work [21].

Proximate and ultimate analyses have been carried out on the chars (Table 2). As can be seen, fixed carbon content (by proximate analysis) and carbon content (by ultimate analysis) increased with char preparation temperature. Differences between both values were larger at lower pyrolysis temperatures, with the ultimate C (which includes both char and residual volatile C in the char) being higher than the fixed carbon. As pyrolysis temperature increased, the proportion of fixed carbon increased and approached ultimate C, indicating the release of hydrogen and oxygen as part of the volatile matter. This was consistent with ultimate analysis also showing a decrease in hydrogen and oxygen contents. Decrease in oxygen content was particularly sharp between 300 and 400 °C. In this temperature range, oxygen release is mainly caused by the scission of alcohol, carbonyl and carboxyl groups, as revealed by FTIR [22]. Losses in hydrogen and oxygen are caused by the scission of weaker bonds at low temperatures and condensation reaction of chars at higher temperatures as made evident by the FTIR results discussed below. Figure 3 summarizes the H/C and O/C ratios of chars. H/C and O/C ratios decreased with pyrolysis temperature, reflecting a greater aromatic and carbonaceous nature of the chars obtained at higher temperatures. Three different regions can be observed in the Van Krevelan diagram in Figure 3. Below 400 °C there was a larger influence of particle size and the drop in H/C ratio was around 2.5 times higher than that of O/C ratio. From 400 to 500 °C there was a decrease in H/C while O/C ratio remained almost constant. Above 500 °C, a linear relationship between both ratios was again observed, with the drop in H/C ratio nearly three times that of O/C ratio. The near-linearity in these relationships is consistent with earlier work [23,41-42] showing that C increases and H and O decreases were proportional to volatile release, and in particular with data on beechwood [43] (shown in Figure SM-1).

SEC profiles of tars produced at different temperatures showed shifts to shorter elution time, indicating larger molecular weights, with increasing pyrolysis temperature. This shows that the increase in tar yield observed between 325 and 400 °C was largely due to the production of tars with larger molecular weight distributions. The difference in SEC chromatograms narrowed above 400 °C in agreement with the stable tar yield values recorded. The SEC chromatograms as a function of temperature are given as supplementary material (Figure SM-2).

3.1.2. Effect of particle size

Particle size had an important effect on product yields (Figure 2). At peak temperatures below 400 °C char yield increased markedly with particle size. Char yields are affected by heating rate and mass transfer resistance within the solid. Volatiles escaping larger particles experience intraparticle reactions to form char before reaching the outer surface of particle, a more noticeable effect for larger particles and at lower temperatures [3,11]. On the other hand, as seen in Figure 2(a), char yields from different particle sizes tended to be similar at the higher end of the temperature range studied. This can be related to the levelling effect of tar secondary reactions on the surface of the bed particles. As for smaller particles the surface area available in the char bed was larger and the tar reacted to a lesser extent within the particles before being released, tar cracking on the bed was significant, leading to relatively larger char and gas production. The comparison of ultimate analysis of chars of different particle sizes (Figure 3) showed that below 400 °C chars derived from biomass of larger particle size showed higher O/C and H/C ratios, while no difference was observed at higher temperatures.

The effect of particle size and pyrolysis temperature on tar yields (Figure 2(b)) was also a result of the balance between tar intraparticle and interparticle reactions. Tar yields decreased with increasing particle size range for temperatures lower than 400 °C as a result of larger extent of reactions within the pyrolysing particles. This trend was reversed at higher temperatures (> 400 °C), with the smaller particles leading to less tar yields. This is associated with the greater surface area available to interact with the volatiles, leading to the occurrence of further tar cracking at high temperatures to form gas [24]. The lower tar yields observed for the 0.212 – 0.5 mm particle size at high temperatures were in agreement with much greater gas yields than those obtained for the two larger particle size ranges (Figure 2(c)). Due to the co-existence of tar intraparticle and interparticle reactions, the effect of particle size on molecular weight distribution was not obvious, as shown in Figure SM-3.

3.2. Char characterization

3.2.1. FTIR Analysis

FTIR spectroscopy enabled identification of changes in biomass and char predominant functional groups as a function of particle size and final pyrolysis temperature. Figure 4 depicts the FTIR spectra for BWC and its chars obtained at final pyrolysis temperatures in the range from 300 to 900 °C. FTIR spectra were complex and showed various peaks representing distinctive functional groups. The main adsorption peaks are assigned in Table 3 based on information from the literature [12,13,25].

The FTIR spectra of the chars changed with pyrolysis temperature, showing structural rearrangements within the forming char. The band at about 3400 cm^{-1} showed a continuous decrease in intensity and broadened with increasing pyrolysis temperature, indicating a disappearance of hydroxyl groups. Nevertheless, this band did not completely disappear at 900 °C, likely due to remaining phenolic groups [15]. The presence of methyl and methylene groups was shown by the appearance of C-H stretching vibration band (2930 cm^{-1}). This band presented a similar trend to the O-H band, with its intensity decreasing rapidly with temperature and becoming almost negligible above 400 °C. Bands related to aromatic C=C vibration and skeletal C=C vibrations (1610 cm^{-1}) were observed in the original BWC and remained present up to the highest pyrolysis temperature studied, which is evidence of the aromatization of the char structure. Skeletal C-C vibration and C-O and O-H bending (1430-1000 cm^{-1}) became smoother with increasing pyrolysis temperature, due to the dehydration and elimination of carbonyl and aliphatic groups during the formation of aromatic units in the chars. At a pyrolysis peak temperature of 600 °C most of these bands disappeared, leading to a more ordered carbon structure. In summary, the main chemical changes during pyrolysis were dehydration, carbonyl group formation and elimination, removal of aliphatic side chains and formation of aromatic char units.

Some differences were observed in the FTIR spectra between chars from BWC of different particle sizes produced at the lower pyrolysis temperatures (comparison between Figures 4(a) and 4(b), also shown in a single figure for each temperature in Figure SM-4). The hydroxyl groups at 3400 cm^{-1}, aliphatic C-H band at 2936 cm^{-1}, bands of C-C skeletal vibration, and C-O and O-H bending all showed greater intensities for larger particle sizes in chars produced at 300 and 350 °C. However, these differences decreased at higher temperatures. This is consistent with ultimate analysis (Figure 3) and char yield data, showing that biomass of larger particle sizes experienced a lesser extent of pyrolysis at lower temperatures, while particle size did not have much effect at higher temperatures.

3.2.2. X-ray diffraction

XRD provided detailed information about the chemical composition and structure of crystalline materials. Stacking of the graphitic basal planes of char crystallites in the low angle region ((002) peak) and radial spread of crystalline structures in the high angle region ((100) peak) are used as indicators of the degree of graphitization. Structural characteristics of the chars produced at pyrolysis temperatures between 300 and 900 °C were established by X-ray diffraction. The X-ray spectra of the chars obtained from two particle size ranges (0.21-0.50 mm and 0.85-1.70 mm) are compared in Figure 5. They illustrate how the crystalline structure of the material changed as pyrolysis temperature increased.

XRD curves of chars obtained from pyrolysis at 300 °C for both particle size ranges analysed showed a cellulose-like pattern [26], which confirms that cellulose is stable at this low pyrolysis temperature [21]. Strong crystalline peaks at around 14^o, 16^o and 23^o and a weak peak at approximately 43^o were identified. When pyrolysis temperature increased from 300 to 325 °C, peaks related to cellulose decreased in intensity and became broader, indicating a loss in crystallinity due to cellulose decomposition. In the case of char obtained at 325 °C from BWC of 0.21-0.50 mm particle size a broad scattering band at around 20^o was registered, which indicates that decomposition of cellulose was almost complete. A slightly higher temperature (350 °C) was necessary to achieve a similar pattern in the case of char produced from particle size in the range 0.85-1.70 mm. This result is in agreement with the slower devolatilisation and chemical changes within larger particles.

Independent of the particle size, chars obtained at temperatures of 400 °C and higher exhibited broad (002) peaks centred at around 23^o with similar amplitude, which indicates a highly disordered structure [6]. At intermediate temperatures, the asymmetry in the (002) peak was related to the presence of aliphatic side chains in the vicinity of char crystallites [6,27]. The peak became more symmetrical with increasing pyrolysis temperature due to the disappearance of these side chains. In addition, (002) peak increased in intensity and became narrower at higher temperatures corresponding to the appearance of a more ordered structure by the formation of turbostratic carbon crystallites at expense of amorphous carbon [28,29]. Between the cellulose crystallite and turbostratic crystallite, X-ray scattering revealed a disintegrated and entirely random carbon phase at intermediate temperatures (350 - 600 °C). Further heating to 700 °C and above gave rise to an additional two-dimensional band at approximately 44^o, attributed to a higher stacking order of polyaromatic

structures. The appearance of this band indicated the presence of crystallites with higher diameters by coalescence of graphene-like layers. Therefore, XRD spectra of chars revealed structural changes towards a more ordered material with increasing temperature, although no significant graphitization was seen at the operating conditions tested.

3.2.3. Raman spectroscopy

Raman spectroscopy was used for the characterisation of ordered and amorphous carbon [30,31]. Parameters obtained from Raman spectra, such as total Raman peak area, the D (defects) and G (graphite) band positions and I_D/I_G band area ratio are used to investigate char structure and its correlation to reactivity. Structural differences in the chars produced at different pyrolysis temperatures were assessed by Raman spectroscopy in the region from 800 to 1800 cm^{-1} (Figure 6). Figure 7 summarizes the total Raman peak area, band positions and I_D/I_G band area ratios obtained from BWC chars from two initial BWC particle sizes (0.22-0.50 mm and 0.85-1.70 mm). Raman spectroscopy has largely been used to study structural features of carbonaceous materials by inferring the extent of graphitization based on the ratio of intensities of the D (defect) band and the G (graphite) band [11,32-35]. However, biomass chars can contain abundant aliphatic structures and O-containing functional groups, which are not likely to be transformed into graphite structures during pyrolysis under the conditions used in this work, i.e. temperatures below 900 °C and holding times shorter than 15 min [33]. Instead, polyaromatic ring systems of varying size present in the char were responsible for primary Raman signals in the range 800-1800 cm^{-1}, with negligible contribution from potential graphite structures. In fact, Raman did not show any definitive sign for the presence of graphitic crystallites in the chars. For these chars, the bands at the D and G positions do not represent the "graphite" or "defect" structures. The G band at around 1590 cm^{-1} can be related to aromatic ring breathing and the D band at around 1350 cm^{-1} can represent aromatic ring systems with more than 6 fused benzene rings [11].

From Figure 7(a), it can be seen that total Raman intensities steadily decreased as pyrolysis temperature increased. This reduction in Raman intensity is explained by the loss of sensitive groups, such as aliphatic and oxygenated groups, and the increase of aromatic structure in the chars, which increases the light absorptivity [11,33,36]. This is consistent with the XRD results and the loss of O content observed by elemental analysis of the chars. In addition, total Raman intensities are higher for the smaller particle sizes, particularly at lower temperatures. As explained above, volatiles experience

significant mass transfer resistance in the larger particles and intraparticle reactions are enhanced, leading to the generation of aromatic structures. The deposited volatiles may not completely polymerise during pyrolysis and thus contribute to form amorphous carbon structures with small fused ring systems (< 6 rings) [11].

D and G band positions as a function of temperature and particle size are shown in Figure 7(b). As can be seen, the G band was slightly displaced towards higher frequencies when temperature increased, which is related to the disappearance of tetrahedral bonds and the formation of trigonal bonds. On the other hand, the D band position shifted to lower frequencies when temperature went from 400 to 700 °C and remained practically steady at higher temperatures, which suggests that the bond-angle disorder decreases [17,37,38]. Position displacements of the D and G bands point to arrangement and ordering of char structure with increasing temperature. The same effects were observed with both particle size ranges of BWC.

From Figure 7(c), the I_D/I_G band area ratio was found to rise for both particle sizes when temperature increased from 400 to 800 °C and remained constant between 800 and 900 °C. The increase in the I_D/I_G ratio can be explained by a growth in number and/or size of crystallites [37,38]. At low pyrolysis temperature, very small crystallites are likely to be present in the char, but they do not contribute to the D band due to their small size and number. The increase in the I_D/I_G ratio with increasing temperature is related to the growth in size and number of aromatic ring systems. This is in agreement with FTIR and XRD results, which also showed an increase in the char structural order with pyrolysis peak temperature. On the other hand, the I_D/I_G band area ratio was lower for chars from BWC 0.85-1.70 mm. This is in agreement with the likely formation of small 3-5 fused ring systems due to secondary reactions of volatiles within large biomass particles, which do not contribute to the D band as explained above.

3.3. Combustion reactivity of chars

The effect of final pyrolysis temperature on combustion reactivity of chars (0.21-0.50 mm) was studied by TGA. Reactivity indices ($T_{50\%}$ and T_{Rmax}) are plotted vs the pyrolysis temperature in Figure 8(a). Both reactivity indices showed a good match and increased with increasing pyrolysis final temperature, indicating a loss of combustion reactivity of chars. This loss of reactivity is related to char structural changes, which in turn depend on pyrolysis conditions [39,40]. Good linear correlations were found between $1/T_{Rmax}$ and the I_D/I_G band area ratio obtained from Raman spectra of

the chars (Figure 8(b)) and between $1/T_{Rmax}$ and La (Figure 8(c)). These findings are consistent with literature reports on a positive correlation between $1/T_{50\%}$ and the bandwidth of second-order Raman microprobe analysis at 2940 cm^{-1} (R^2 = 0.96) in cellulose-derived chars [35]. The greater I_D/I_G band area ratio and La were due to the growth in size and number of aromatic ring systems and crystallites with temperature, which had a direct negative impact on char reactivity.

The presence of oxygen-containing functional groups and aliphatic side chains in the char is known to be related to the availability of active sites on carbon surface and enhanced reactivity [3,5,6,11,27]. Ultimate analysis, FTIR, XRD and Raman results revealed the loss of these functional groups with increasing temperature, which is consistent with the decrease in combustion reactivity. Moreover, FTIR, XRD and Raman results showed an increase in size and number of aromatic ring systems, leading to a more ordered char structure. Carbon atoms bonded to heteroatoms, nascent sites, and edges or dislocations in the crystallites are chemically unsaturated and more prone to react [40]. On the contrary, the basal carbon atoms in the interior of polycyclic condensed aromatic structure of char are inert, which leads to less reactivity [3].

4. Conclusions

Beechwood chip samples in three particle size ranges (0.21-0.50 mm, 0.85-1.70 mm and 2.06-3.15 mm) were pyrolysed in a laboratory scale fixed bed reactor to various final temperatures within the range of 300 to 900 °C. As expected, tar and gas yields increased with temperature, while solid residue yield decreased. Changes were particularly sharp between 300 and 500 °C, levelling off at higher temperatures.

Biomass particle size had a significant impact on product yields in the lower temperature region. Intraparticle reactions led to decreasing tar and gas yields and increasing char yield with particles size at temperatures lower than 400 °C. However, at higher temperatures the effect of the larger surface area provided by small particle sizes, which is available for tar cracking and condensation reactions on the bed, became predominant. Reactions in the char bed resulted in similar char yields for all particle sizes and an increase in gas at the expense of tar yield due to enhanced cracking for the smaller particles.

Increasing pyrolysis temperatures led to a loss of O-containing functional groups and aliphatic side chains and a growth in size and number of aromatic ring systems. This produced more ordered char structures as observed by FTIR, XRD and Raman spectroscopies. However, no significant

graphitization of the chars took place. Instead, XRD indicated the formation of turbostratic carbon crystallites.

Slightly higher temperatures were needed to completely decompose the cellulose structure when the biomass particle size increased as observed by XRD. Enhanced intraparticle reactions in large particles gave rise to amorphous carbon structures with small fused ring systems, which Raman spectra revealed that grew in size and number as pyrolysis temperature increased. These structural changes undergone by the biomass chars led to a decrease in the combustion reactivity of chars with pyrolysis temperature.

Acknowledgements

This research was supported by the National Natural Science Foundation of China (No. 51661145010). Funding from the Research Fund for Coal and Steel of the European Union through projects RFSR-CT-2009-00004 and RFSP-CT-2014-00003, and EPSRC, UK, (Grant No. EP/K014676/1) is gratefully acknowledged. CB is grateful to the Spanish Ministry of Economy and Competitiveness (MINECO) for funding his Ramon y Cajal contract (RYC-2011-09202).

References

[1] T. Fouilland, J.R. Grace and N. Ellis, Recent advances in fluidized bed technology in biomass processes, Biofuels, 1, (2014) 409-433.

[2] A. Kumar, D.D. Jones and M.A. Hanna, Thermochemical Biomass Gasification: A Review of the Current Status of the Technology, Energies, 2, (2009) 556-581.

[3] M. Asadullah, S. Zhang and C.-Z. Li, Evaluation of structural features of chars from pyrolysis of biomass of different particle sizes, Fuel Process. Technol., 91, (2010) 877-88.

[4] M. Asadullah, S. Zhang, Z. Min, P. Yimsiri and C.Z. Li, Importance of Biomass Particle Size in Structural Evolution and Reactivity of Char in Steam Gasification, Ind. Eng. Chem. Res., 48,(2009) 9858-9863.

[5] C. Di Blasi, Combustion and gasification rates of lignocellulosic chars, Prog. Energy Combust. Sci., 35, (2009) 121-140.

[6] M. Guerrero, M.P. Ruiz, á. Millera, M.U. Alzueta and R. Bilbao, Characterization of Biomass Chars Formed under Different Devolatilization Conditions: Differences between Rice Husk and Eucalyptus, Energy Fuels, 22, (2008) 1275-1284.

[7] O. Onay, Influence of pyrolysis temperature and heating rate on the production of bio-oil and char from safflower seed by pyrolysis, using a well-swept fixed-bed reactor, Fuel Process.Technol., 88, (2007) 523-531.

[8] B. Fidalgo, C. Berrueco and M. Millan, Chars from agricultural wastes as greener fuels for electric arc furnaces, J Anal. Appl. Pyrolysis, 113, (2015) 274-280.

[9] W.J. Liu, H. Jiang and H.Q. Yu, Development of Biochar-Based Functional Materials: Toward a Sustainable Platform Carbon Material, Chem. Rev., 115, (2015) 12251-12285.

[10] A. Sharma, V. Pareek and D. Zhang, Biomass pyrolysis—A review of modelling, process parameters and catalytic studies, Renew. Sust. Energ. Rev., 50, (2015) 1081-1096.

[11] M. Asadullah, S. Zhang, Z. Min, P. Yimsiri and C.Z. Li, Effects of biomass char structure on its gasification reactivity, Bioresour. Technol., 101, (2010) 7935-7943.

[12] K. Bilba and A. Ouensanga, Fourier transform infrared spectroscopic study of thermal degradation of sugar cane bagasse, J. Anal. Appl. Pyrolysis, 38, (1996) 61-73.

[13] P. Fu, S. Hu, J. Xiang, L. Sun, P. Li, J. Zhang and C. Zheng, Pyrolysis of Maize Stalk on the Characterization of Chars Formed under Different Devolatilization Conditions, Energy Fuels, 23,(2009)

4605-4611.

[14] R. Kandiyoti, A.A. Herod, and K. Bartle, Solid Fuels and Heavy Hydrocarbon Liquids, Elsevier Science & Technology, (2006).

[15] R.K. Sharma, J.B. Wooten, V.L. Baliga and M.R. Hajaligol, Characterization of chars from biomass-derived materials: pectin chars, Fuel, 80, (2001) 1825-1836.

[16] R.K. Sharma, J.B. Wooten, V.L. Baliga, X. Lin, W. Geoffrey Chan and M.R. Hajaligol, Characterization of chars from pyrolysis of lignin, Fuel, 83, (2004) 1469-1482.

[17] S. Yamauchi and Y. Kurimoto, Raman spectroscopic study on pyrolyzed wood and bark of Japanese cedar: temperature dependence of Raman parameters, J. Wood Sci., 49, (2003) 235-240.

[18] R.K. Sharma, J.B. Wooten, V.L. Baliga, M.S. and M.R. Hajaligol, Characterization of Char from the Pyrolysis of Tobacco, J. Agric. Food Chem., 50, (2002) 771-783.

[19] M. Cordella, C. Berrueco, F. Santarelli, N. Paterson, R. Kandiyoti and M. Millan, Yields and ageing of the liquids obtained by slow pyrolysis of sorghum, switchgrass and corn stalks, J. Anal. Appl. Pyrolysis, 104, (2013) 316-324.

[20] M. Kumar, R.C. Gupta and T. Sharma, X-ray diffraction studies of Acacia and Eucalyptus wood chars, J. Mater. Sci., 28, (1993) 805-810.

[21] J. Yu, N. Paterson, J. Blamey and M. Millan, Cellulose, xylan and lignin interactions during pyrolysis of lignocellulosic biomass, Fuel, 191, (2017) 140-149.

[22] F.-X. Collard and J. Blin, A review on pyrolysis of biomass constituents: Mechanisms and composition of the products obtained from the conversion of cellulose, hemicelluloses and lignin, Renew. Sust. Energ. Rev., 38, (2014) 594-608.

[23] R. Volpe, A. Messineo, M. Millan, M. Volpe and R. Kandiyoti, Assessment of olive wastes as energy source: pyrolysis, torrefaction and the key role of H loss in thermal breakdown, Energy, 82, (2015) 119-127.

[24] F. Dabai, N. Paterson, M. Millan, P. Fennell and R. Kandiyoti, Tar Formation and Destruction in a Fixed-Bed Reactor Simulating Downdraft Gasification: Equipment Development and Characterization of Tar-Cracking Products, Energy Fuels, 24, (2010) 4560-4570.

[25] B. Chen, D. Zhou and L. Zhu, Transitional adsorption and partition of nonpolar and polar aromatic contaminants by biochars of pine needles with different pyrolytic temperatures, Environ. Sci. Technol., 42, (2008) 5137-5143.

[26] X. Ju, M. Bowden, E.E. Brown and X. Zhang, An improved X-ray diffraction method for cellulose crystallinity measurement, Carbohydr. Polym., 123, (2015) 476-481.
[27] L. Lu, Coal char reactivity and structural evolution during combustion-factors influencing blast furnace pulverized coal injection operation, Metall. Mater. Trans. B, 32, (2001) 811-820.
[28] A.K. Kercher and D.C. Nagle, Microstructural evolution during charcoal carbonization by X-ray diffraction analysis, Carbon, 41, (2003) 15-27.
[29] O. Paris, C. Zollfrank and G.A. Zickler, Decomposition and carbonisation of wood biopolymers—a microstructural study of softwood pyrolysis, Carbon, 43, (2005) 53-66.
[30] S. Dong, P. Alvarez, N. Paterson, D.R. Dugwell and R. Kandiyoti, Study on the Effect of Heat Treatment and Gasification on the Carbon Structure of Coal Chars and Metallurgical Cokes using Fourier Transform Raman Spectroscopy, Energy Fuels, 23, (2013) 1651-1661.
[31] S. Dong, N. Paterson, S.G. Kazarian, D.R. Dugwell and R. Kandiyoti, Characterization of Tuyere-Level Core-Drill Coke Samples from Blast Furnace Operation, Energy Fuels, 21, (2007) 3446-3454.
[32] O. Beyssac, B. Goffé, J.-P. Petitet, E. Froigneux, M. Moreau and J.-N. Rouzaud, On the characterization of disordered and heterogeneous carbonaceous materials by Raman spectroscopy, Spectrochim. Acta. A Mol. Biomol. Spectrosc., 59, (2003) 2267-2276.
[33] X. Guo, L.T. Hui, S. Zhang and C.Z. Li, Changes in Char Structure during the Gasification of a Victorian Brown Coal in Steam and Oxygen at 800 °C, Energy Fuels, 22, (2008) 4034-4038.
[34] X. Li, J. Hayashi and C. Li, FT-Raman spectroscopic study of the evolution of char structure during the pyrolysis of a Victorian brown coal, Fuel, 85, (2006) 1700-1707.
[35] A. Zaida, E. Bar-Ziv, L.R. Radovic and Y.-J. Lee, Further development of Raman Microprobe spectroscopy for characterization of char reactivity, P. Combust. Inst., 31, (2007) 1881-1887.
[36] O. Ito, Diffuse reflectance spectra of coals in the UV-visible and near-IR regions, Energy Fuels, 6, (1992) 662-665.
[37] R.O. Dillon, J.A. Woollam and V. Katkanant, Use of Raman scattering to investigate disorder and crystallite formation in as-deposited and annealed carbon films, Phys. Rev. B, 29, (1984) 3482-3489.
[38] J.T. Jiu, H. Wang, C.B. Cao and H.S. Zhu, The effect of annealing temperature on the structure of diamond-like carbon films by electrodeposition technique, J. Mater. Sci., 34, (1999) 5205-5209.
[39] A. Cousins, N. Paterson, D.R.D. And and R. Kandiyoti, An Investigation of the Reactivity of Chars

Formed in Fluidized Bed Gasifiers: The Effect of Reaction Conditions and Particle Size on Coal Char Reactivity, Energy Fuels, 20, (2006) 197-210.

[40] S.Y. Zhang, J.F. Lu, J.S. Zhang and G.X. Yue, Effect of Pyrolysis Intensity on the Reactivity of Coal Char, Energy Fuels, 22, (2008) 3213-3221.

[41] P. Fu, S. Hu, L. Sun, J. Xiang, T. Yang, A. Zhang and J. Zhang, Structural evolution of maize stalk/char particles during pyrolysis, Bioresource Technology, 100, (2009) 4877.

[42] R. Xiao and W. Yang, Influence of temperature on organic structure of biomass pyrolysis products, Renewable Energy, 50, (2013) 136.

[43] K. Zeng, D.P. Minh, D. Gauthier, E. Weiss-Hortala, A. Nzihou and G. Flamant, The effect of temperature and heating rate on char properties obtained from solar pyrolysis of beech wood, Bioresource Technology, 182, (2015) 114.

Table 1. Proximate and ultimate analysis of the BWC sample (%).

Sample	Beechwood
Proximate analysis[a] (%)	
Moisture	11.6
Ash	0.5
Volatile Matter	75.0
Fixed Carbon	12.9
Ultimate analysis[b] (%)	
Carbon	45.5
Oxygen (by difference)	48.1
Hydrogen	6.1
Nitrogen	0.08
Sulphur	0.21

[a] as used basis; [b] dry ash-free basis

Table 2. Proximate and ultimate analysis of BWC solid residues obtained at different pyrolysis temperatures. Particle size: 0.85-1.70 mm.

Pyrolysis temperature (℃)	Proximate analysis (wt.%)		Ultimate analysis (wt.%)[a]		
	Volatile Matter[a]	Fixed Carbon[a]	C	H	O
300	79.3	20.7	54.2	5.5	33.2
325	66.3	33.8	55.4	5.1	32.2
350	65.0	35.0	59.5	4.4	28.2
400	55.2	44.8	67.9	3.7	18.1
450	50.3	49.7	66.1	3.4	18.3
500	44.8	55.2	66.1	3.1	17.4
600	37.2	62.9	69.3	2.5	15.3
700	34.1	65.9	72.0	1.6	9.6

[a] Dry ash-free basis; O was calculated by difference.

Table 3. FTIR signal assignment according to [11, 13 and 24].

Frequency (cm^{-1})	Atomic groups and structures
~ 3400	O-H stretching vibration
~ 2930	C–H stretching vibrations
~ 1708	C=O stretching vibration from esters
~ 1610	C=O stretching vibration conjugated to the aromatic ring, aromatic ring vibration
~ 1512	C=C ring stretching vibration of lignin
~ 1460	Aromatic skeletal vibration combined with C-H in plane deformation
1320	Esters, epoxides and acyclic C-O-C groups conjunction with C=C in olefinic or aromatic structures
~ 1160	C–O stretching in six-membered ring ether structures
1000 ~ 1100	C–O vibrations in primary and secondary C-OH, related to cellulosic components
730 ~ 900	aromatic C-H out of plane deformation

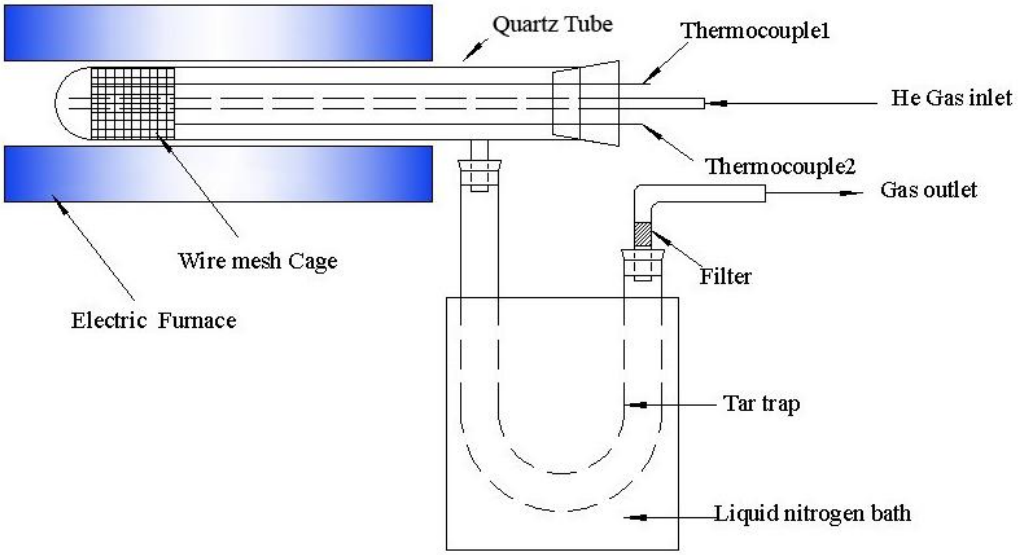

Figure 1. Fixed bed reactor system adapted from a Gray-King configuration.

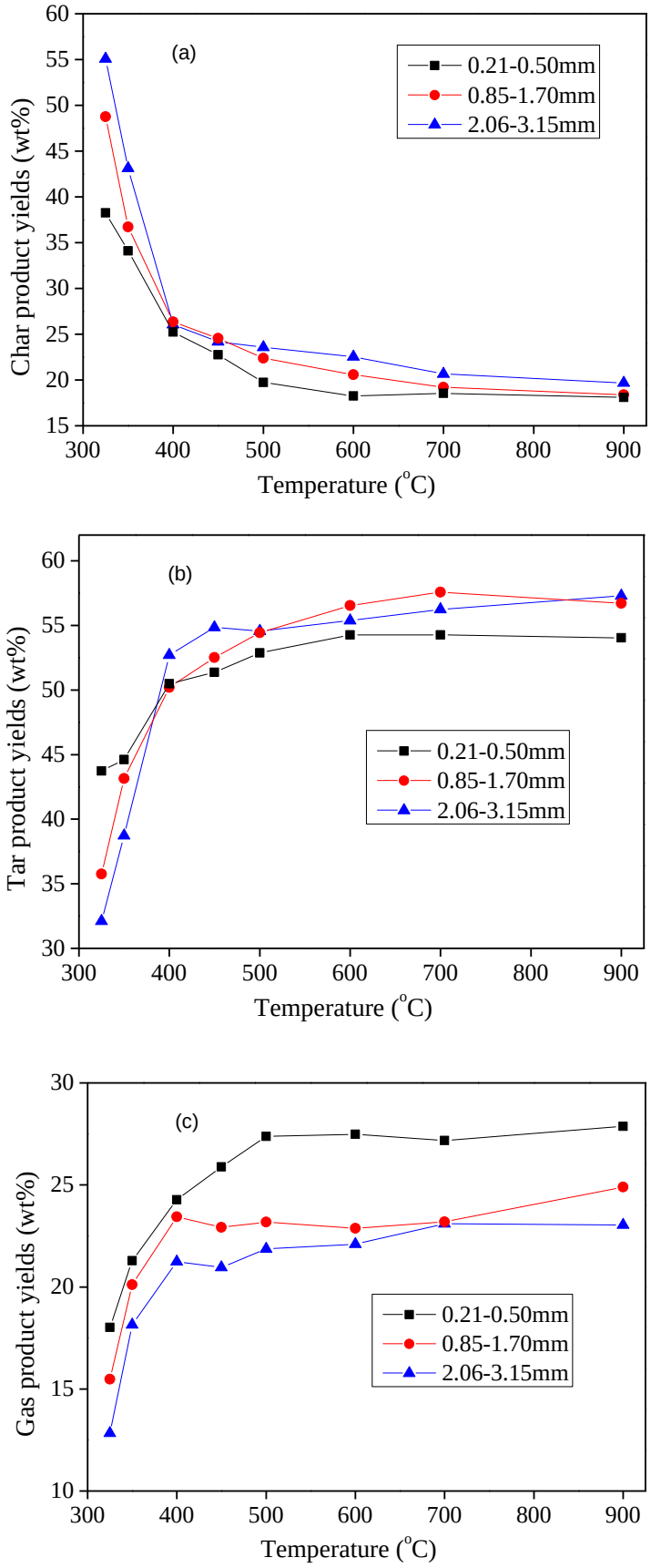

Figure 2. Effect of temperature and particle size on: (a) char yield; (b) tar yield; and, (c) gas yield.

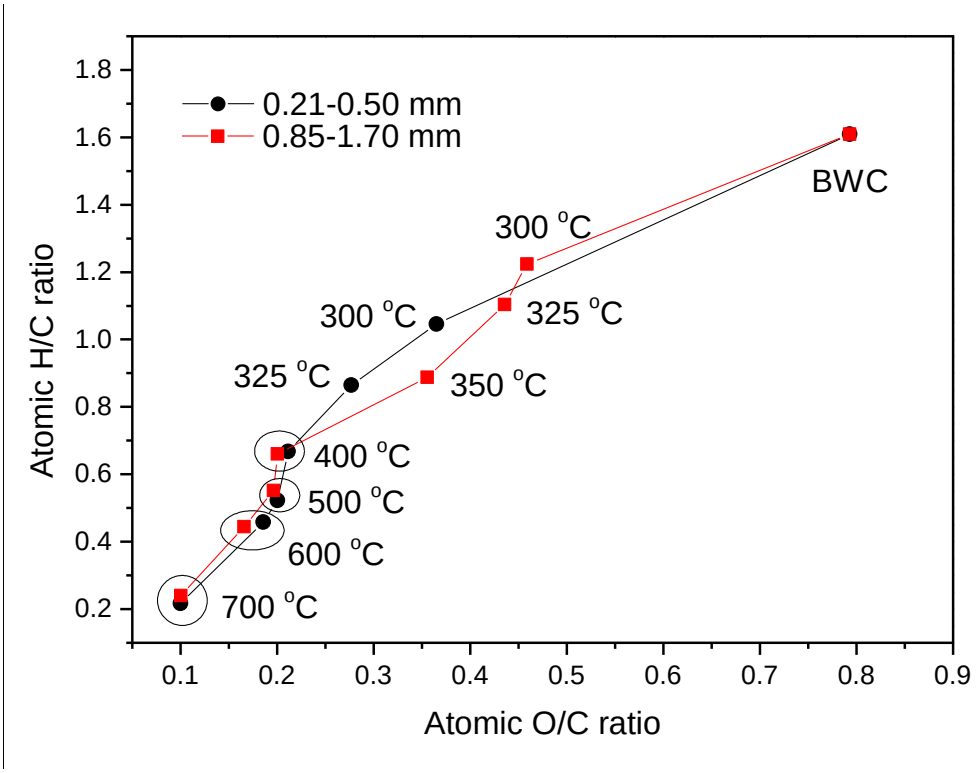

Figure 3. Van Krevelan diagram for BWC and the chars at different temperatures.

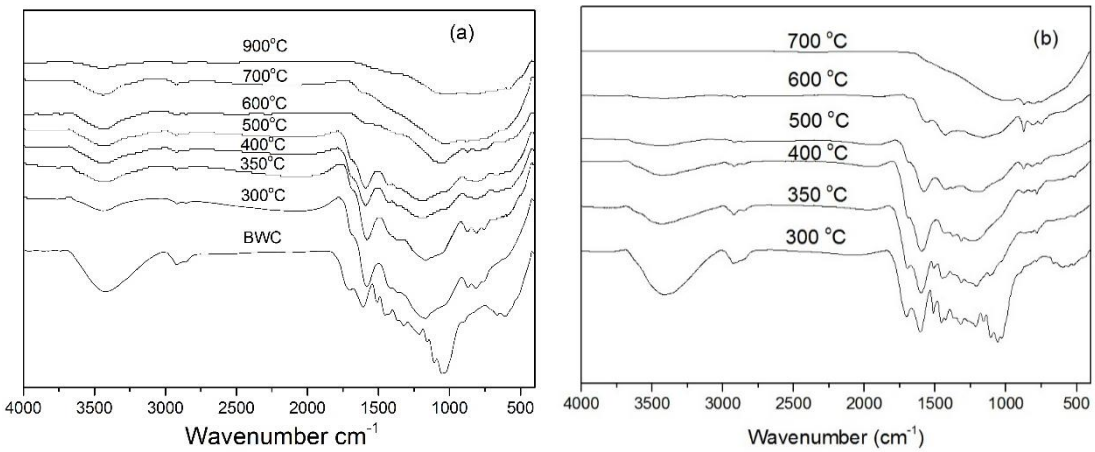

Figure 4. FTIR spectra of beech wood chips and its chars obtained at different pyrolysis temperatures.

Particle size: (a) 0.21 – 0.50 mm (b) 0.85-1.70 mm.

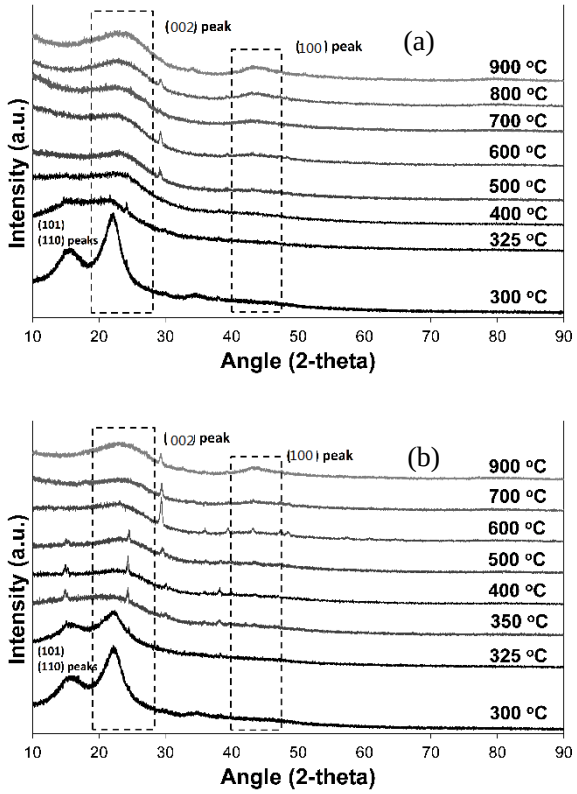

Figure 5. XRD patterns of chars obtained at different pyrolysis temperatures and particle size:

(a) 0.21 – 0.50 mm, (b) 0.85 – 1.70 mm.

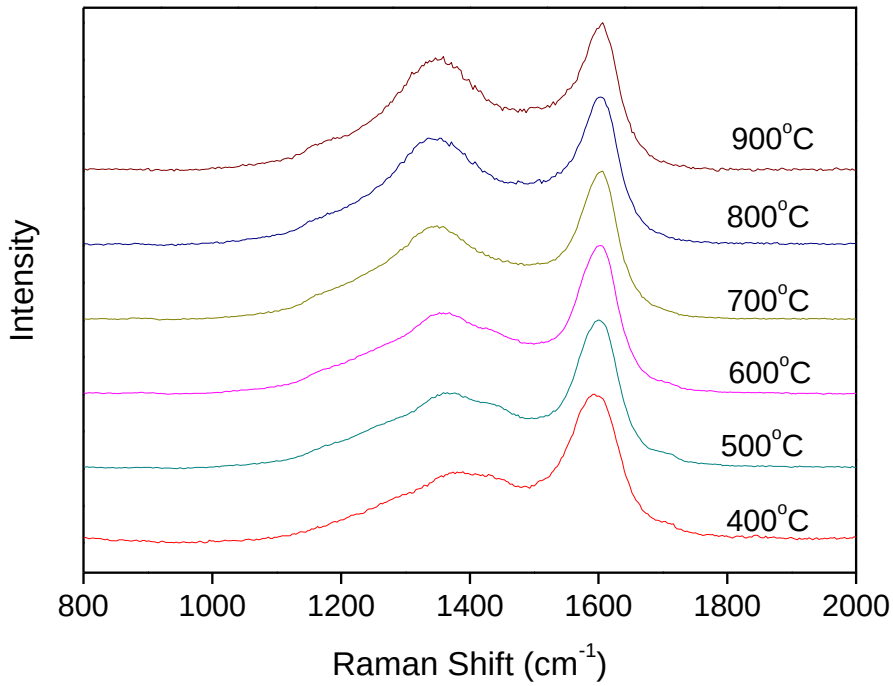

Figure 6. Raman spectra for chars produced at different pyrolysis temperature (particle size: 0.212 - 0.5 mm).

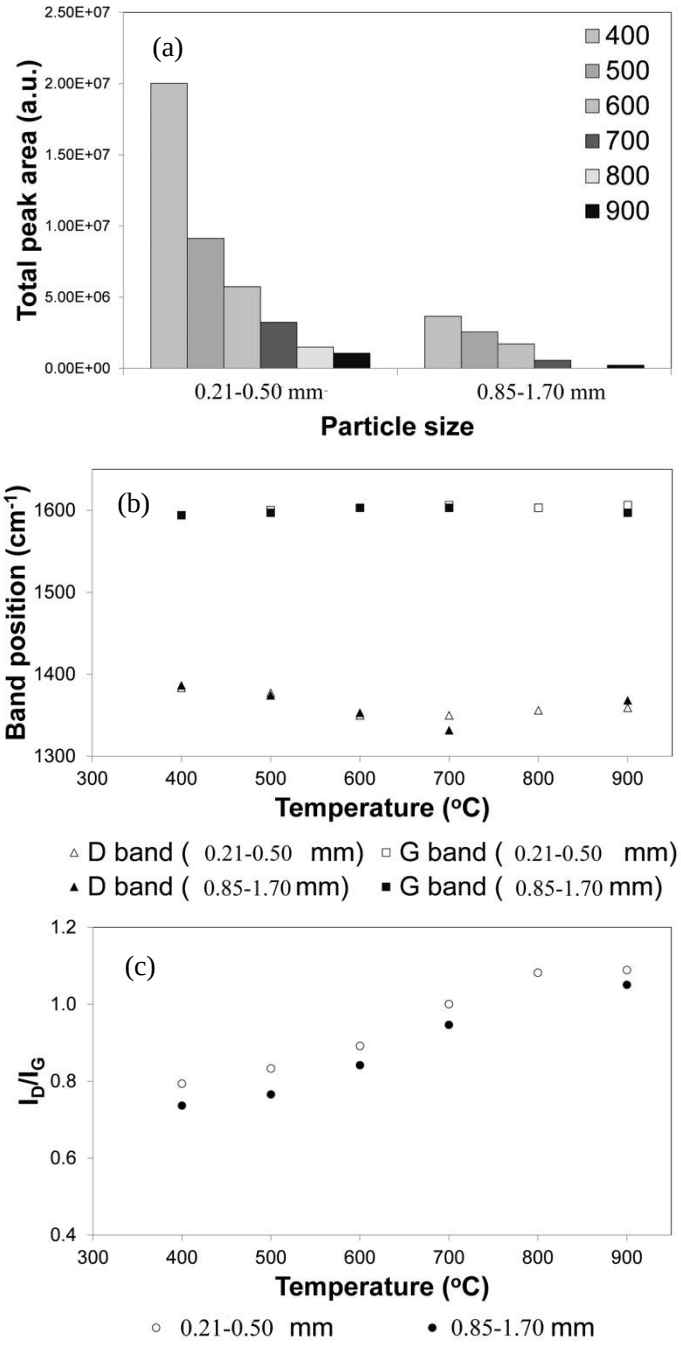

Figure 7. Raman parameters of chars obtained at different pyrolysis temperatures and particle sizes: (a) Total Raman peak area; (b) Band position; (c) Ratio of band peak areas I_D/I_G.

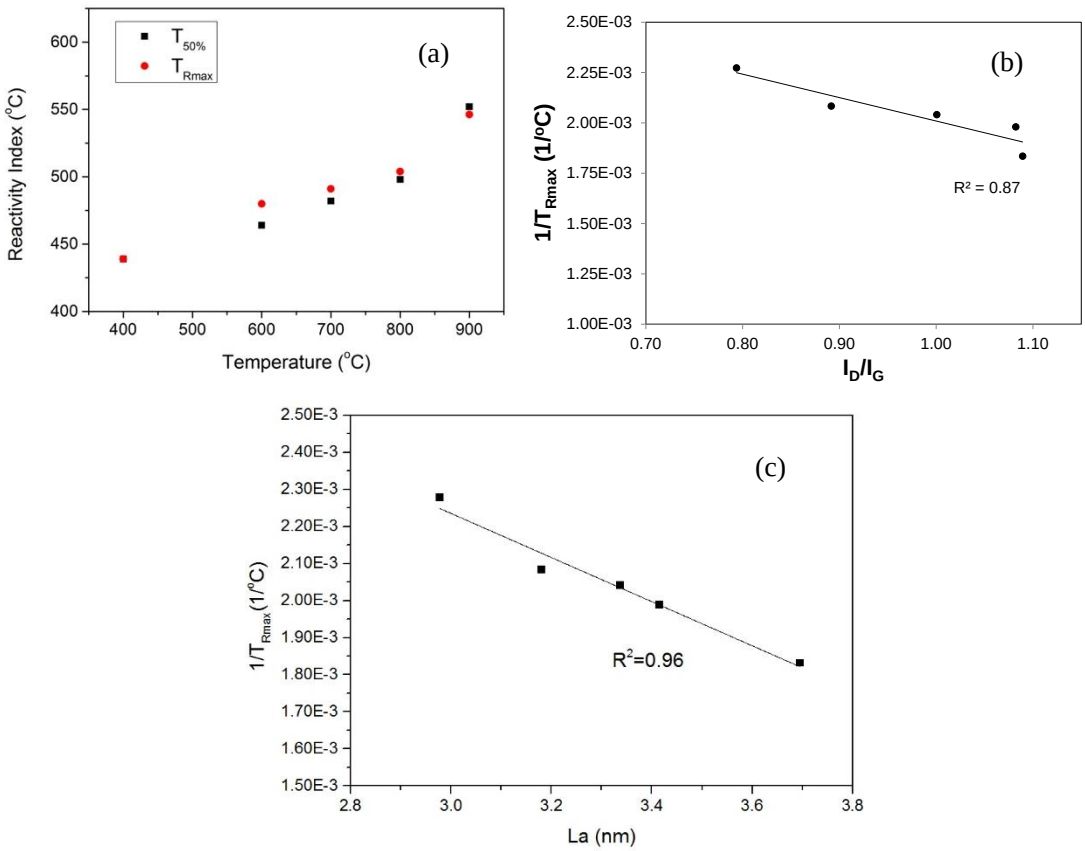

Figure 8. (a) Influence of final pyrolysis temperature on combustion reactivity indices of BWC chars; (b) Correlation between $1/T_{Rmax}$ and I_D/I_G ratio obtained from Raman spectra. (c) Correlation between $1/T_{Rmax}$ and La (nm) obtained from XRD. Particle size: 0.21 – 0.50 mm.

Supplementary Materials

Influence of temperature and particle size on structural characteristics of chars from Beechwood pyrolysis

Jie Yu[1,2], Lushi Sun[1,2], César Berrueco[2,3], Beatriz Fidalgo[2,4], Nigel Paterson[2], Marcos Millan[2*]

[1] State Key Laboratory of Coal Combustion, Huazhong University of Science and Technology, Wuhan, Hubei 430074, China

[2] Department of Chemical Engineering, Imperial College, London SW7 2AZ, UK

[3] Current Address: Catalonia Institute for Energy Research, IREC. C/ Marcel·lí Domingo, 2. 43007 Tarragona, Spain

[4] Current Address: Bioenergy and Resource Management Centre, Cranfield University, Cranfield MK43 0AL, UK

* Corresponding author. Tel.: +44(0)2079541633

E-mail address: marcos.millan@imperial.ac.uk

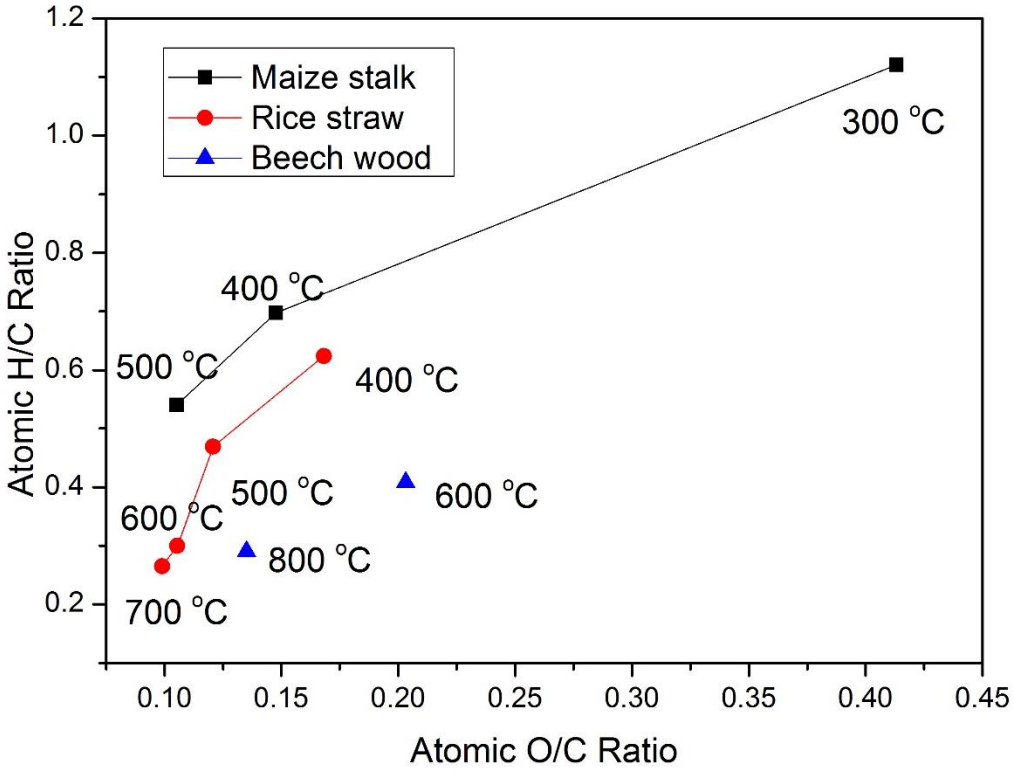

Figure SM-1. Van Krevelan diagram for the chars of maize stalk [1], rice straw [2] and beechwood [3] at different temperatures.

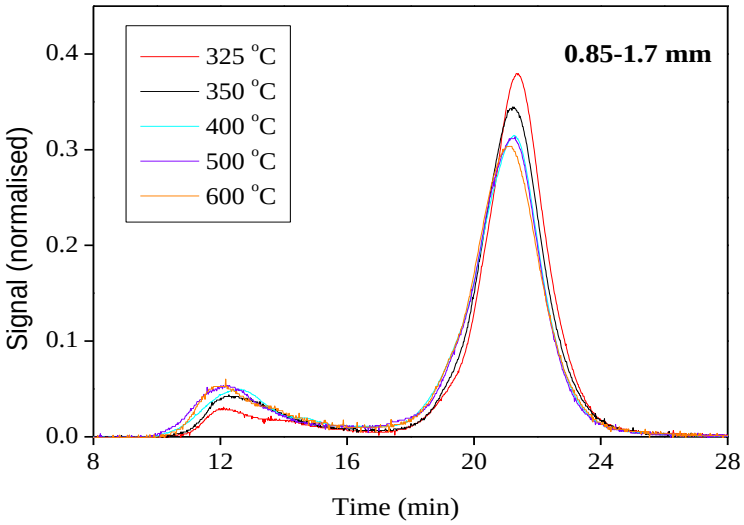

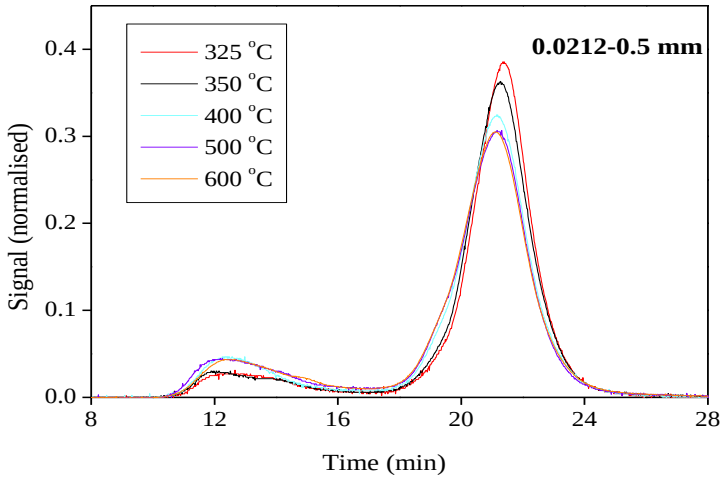

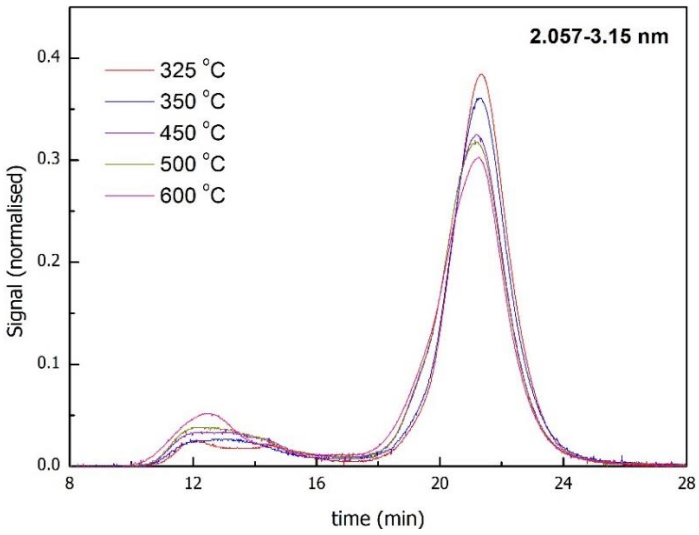

Figure SM-2. SEC profile of tars produced at different pyrolysis temperatures for three BWC particle size ranges.

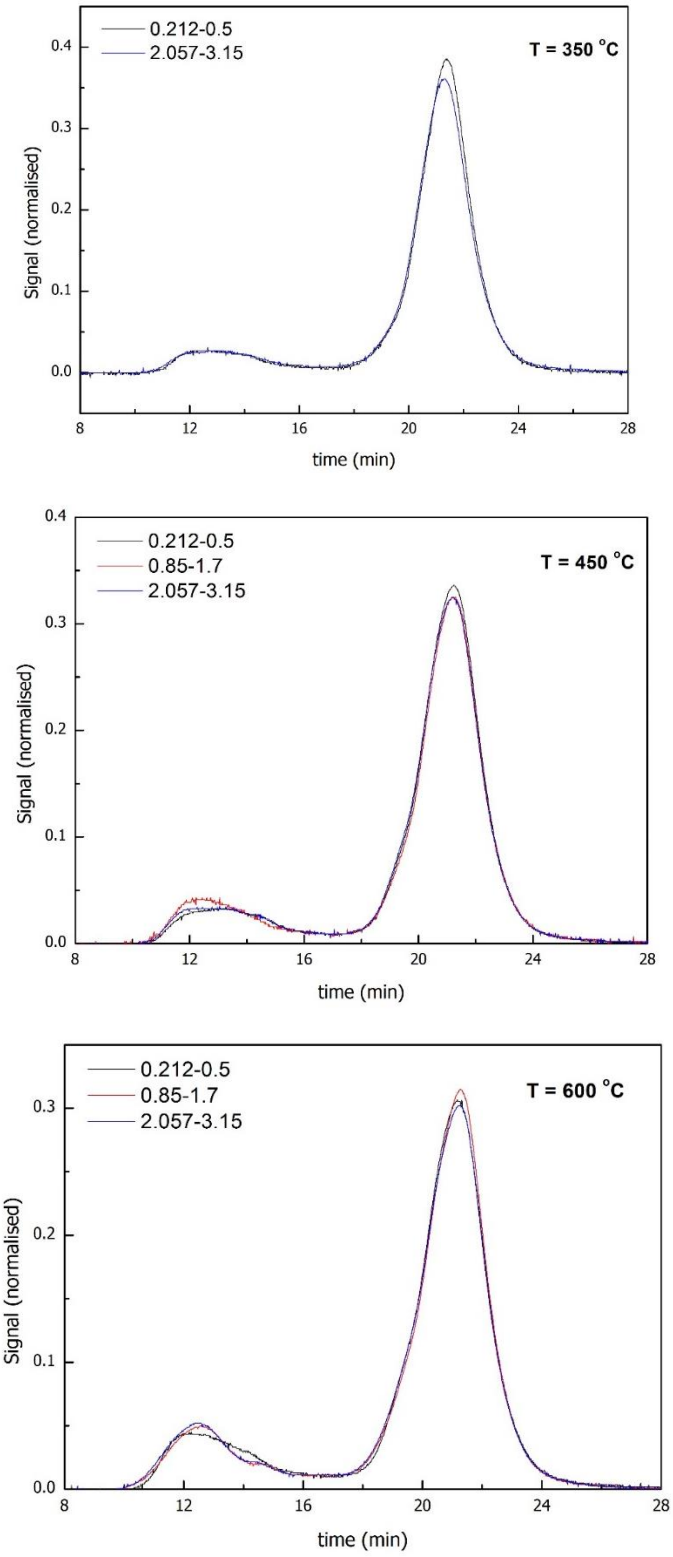

Figure SM-3. SEC profile of tars produced from different particle sizes of BWC for three different pyrolysis temperatures.

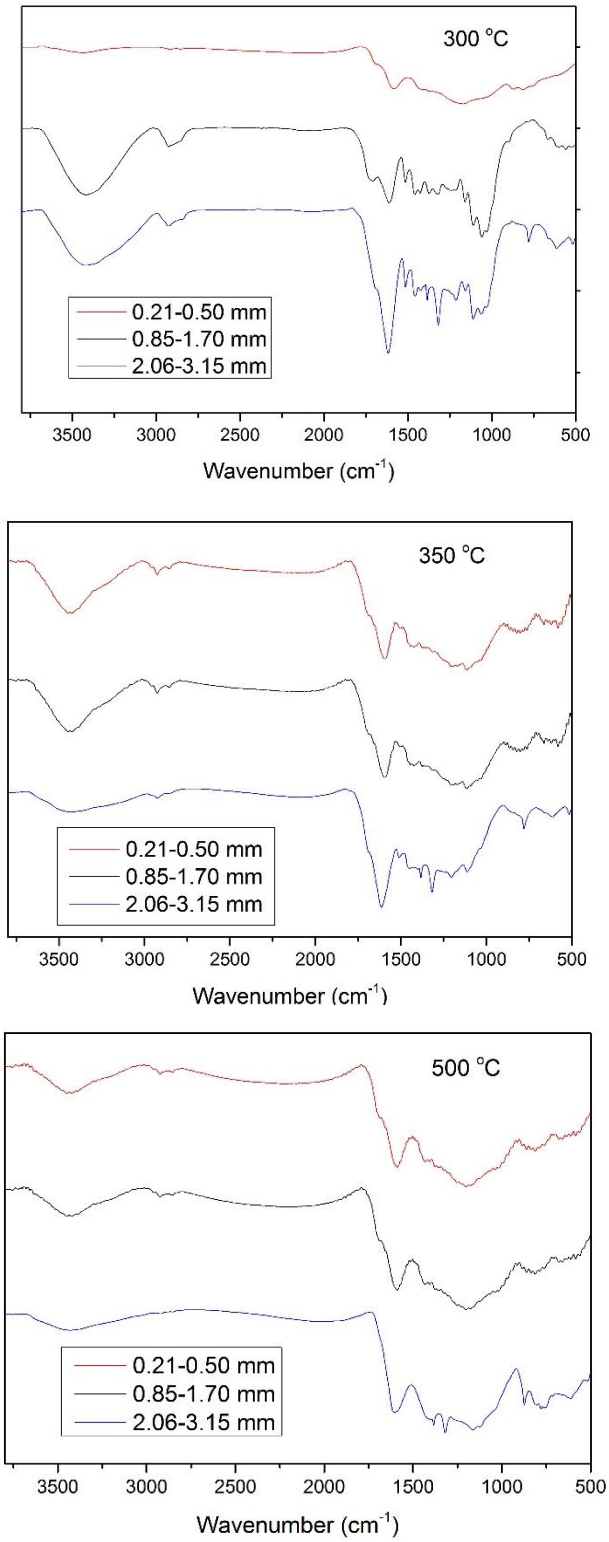

Figure SM-4. FTIR of chars produced from BWC of different particle size at different temperatures.

References

[1] P. Fu, S. Hu, L. Sun, J. Xiang, T. Yang, A. Zhang and J. Zhang,Structural evolution of maize stalk/char particles during pyrolysis, *Bioresource Technology*, 100, (2009) 4877.

[2] R. Xiao and W. Yang,Influence of temperature on organic structure of biomass pyrolysis products, *Renewable Energy*, 50, (2013) 136.

[3] K. Zeng, D.P. Minh, D. Gauthier, E. Weiss-Hortala, A. Nzihou and G. Flamant,The effect of temperature and heating rate on char properties obtained from solar pyrolysis of beech wood, *Bioresource Technology*, 182, (2015) 114.